Date of Issue: December 31, 1986
Distribution Category: UC-4, UC-25

Y--2378

DE87 004552

CARBON MONOXIDE REACTION WITH LIQUID URANIUM-NIOBIUM ALLOYS

R. H. Reiner
C. E. Holcombe, Jr.

Metals and Ceramics Department
Development Division

December 1986

Prepared by the
Oak Ridge Y-12 Plant
P.O. Box Y, Oak Ridge, Tennessee 37831
operated by
MARTIN MARIETTA ENERGY SYSTEMS, INC.
for the
U.S. DEPARTMENT OF ENERGY
under contract DE-AC05-84OR21400

CONTENTS

SUMMARY

The reaction kinetics of liquid uranium and uranium-niobium (U-Nb) alloys with carbon monoxide (CO) were determined as functions of niobium composition, exposure time, exposure temperature, CO pressure, and specific surface area of the liquid-vacuum interface. The experimental results indicate that this reaction is a major source of carbon contamination during foundry casting of uranium–2 wt % niobium alloys (Y-12 process number 3036), being at least ten times as important as the yttria coating reaction with graphite. Uranium alloy reactions with CO decrease with increasing niobium concentration, indicating that most CO-produced carbon contamination in 3036 castings occurs from reaction with uranium feed. The reaction kinetics of CO with U-Nb alloys are consistent with CO diffusion at the liquid-vacuum interface as the rate-determining step.

INTRODUCTION

The melting and casting of high-purity uranium alloys is a mature, well-documented technology.[1] The major sources of contamination during melting are alloy interactions with the containment crucible and with the furnace environment. In the preparation of small quantities of ultrahigh-purity material, alloy-crucible interactions are minimized by the use of reaction-resistant ceramic oxides, such as thoria, beryllia, or yttria. Alloy interactions with the environment are minimized by operating the furnace at high vacuum.

While this technology is quite useful in the preparation of small castings, control of uranium contaminants in foundry castings remains an important concern because of the casting size and the costs associated with eliminating contaminants. In particular, carbon contamination from the graphite components (crucibles, molds, and rods) limits the purity of uranium castings. Graphite is currently used in foundry casting of uranium–2 wt % niobium (U–2 wt % Nb) alloy (3036 castings) because it is easy to machine, has good thermal-shock resistance, and is relatively inexpensive. When protected by a painted ceramic coating, graphite components are reusable and more economical than any ceramic substitutes tested thus far.

Graphite components in direct contact with uranium or uranium alloys are coated with a ceramic paint (usually yttria or zirconia) to minimize carbon contamination. When the protective coatings are properly applied, uranium does not contact the graphite; the following uranium-graphite reaction is prevented:

$$U(1) + C(s) \longrightarrow UC(s) \ . \qquad (1)$$

Although the coating prevents direct uranium-carbon contact, some carbon contamination from the coating still occurs because the paint is applied with a carbon-containing binder and because the protective oxide coatings are slowly reduced by graphite at foundry temperatures. For example, the yttria coating reacts with graphite to make carbon monoxide (CO):

$$Y_2O_3(s) + 7C(s) \longrightarrow 2YC_2(s) + 3CO(g) \ . \qquad (2)$$

The CO produced by Reaction (2) then reacts with the uranium alloy to produce uranium carbide (UC),

$$CO(g) + 2U(1) \longrightarrow UC(s) + UO(s) \ , \qquad (3)$$

or niobium carbides (NbC, Nb_2C),

$$CO(g) + 2Nb(s) \longrightarrow NbC(s) + NbO(s) \ , \qquad (4)$$

$$CO(g) + 3Nb(s) \longrightarrow Nb_2C(s) + NbO(s) \ . \qquad (5)$$

Reaction (2) and similar coating-graphite reactions have been studied by Holcombe.[2] The extent of carbon contamination depends on the melt temperature, exposure time, and ratio of coated crucible surface area to mass of molten alloy. Holcombe's experiments indicate that, for typical foundry conditions, approximately 10% of the yttria coating reacts with the graphite crucible. For coated surface areas and liquid volumes in foundry melts, if all the CO generated by Reaction (2) subsequently contaminated the molten alloy, carbon concentrations would increase by 2 ppm.

Since carbon concentrations in foundry castings typically increase by 15 to 60 ppm during furnacing, there is probably another source of carbon contamination in addition to the coating-graphite reaction. This additional carbon source is assumed to be CO produced from air inleakage.[3] At foundry operating temperatures, oxygen and water vapor from air inleakage can react with the graphite components to generate additional CO:

$$O_2(g) + 2C(s) \longrightarrow 2CO(g) \cdot \qquad (6)$$

and

$$H_2O(g) + C(s) \longrightarrow CO(g) + H_2(g) \ . \qquad (7)$$

Any CO generated by Reactions (6) and (7) can subsequently react with molten uranium by Reaction (3).

The reaction mechanism for CO contamination produced by coating reaction with graphite [Reaction (2)] is different from that for CO contamination produced by air inleakage [Reactions (6) and (7)]. The CO generated by Reaction (2) enters the melt at the crucible-liquid interface, whereas CO generated by Reactions (6) and (7) reacts with the alloy at the liquid-vacuum interface. Since both reactions are surface area dependent, the contributions of each should scale as the appropriate interface ratio of surface to melt volume. However, CO contamination produced by air inleakage should be strongly dependent on the furnace vacuum since the CO concentration at the melt-vacuum interface is pressure dependent. Carbon contamination from the coating-graphite reaction, on the other hand, probably depends only on the kinetics of Reactions (2) and (3) at the coating-liquid interface.

A parametric study of the reaction kinetics was conducted to determine the importance of the U-Nb alloy reactions with CO to foundry carbon contamination. In the study, the alloy carbon gain after furnacing was determined as functions of alloy composition, [Nb], furnace temperature, T, furnace exposure time, t, CO partial pressure, [CO], and specific surface area of the melt-vacuum interface, (S/V). In addition, the relative importance of coating reactions and inleakage as sources for CO contamination were determined for typical foundry furnacing conditions. Subsequent sections of this report present the experimental procedures used to conduct this study, the results of the parametric studies and the foundry furnacing simulations, an analysis of the contamination mechanisms, the implications to the production of the U–2 wt % Nb alloy, and the conclusions drawn from the study.

EXPERIMENTAL PROCEDURE

Kinetic measurements of the liquid alloy reactions with CO were made by controlled exposure of known-purity uranium and uranium-niobium (U-Nb) alloys for a specific time, temperature, CO pressure, and specific surface area of the liquid-vacuum interface. Uranium and U–6 wt % Nb alloy samples of known carbon content were ultrasonically cleaned in 50% nitric acid, rinsed in distilled water, and then rinsed in ethanol to remove surface contamination. Each sample was then weighed into a plasma-sprayed yttria crucible and loaded into a noncarbon, high-vacuum furnace. The sample was heated to temperature at a background pressure less than 10^{-5} torr (maintained by vacuum ion and sorption pumps). After the sample had equilibrated at the desired temperature (between 15 to 30 min), the exposure was initiated by adding CO through a variable leak valve. During the exposure, CO pressure and uranium temperature were monitored by a capacitance manometer and an optical pyrometer, respectively, and manually controlled to within 0.2% of the desired values. The exposure was terminated by closing the leak valve. The sorption pumps removed 99% of the CO within 1 min. After 15 min, the background pressure was less than 10^{-6} torr and the furnace was cooled. After cooling under vacuum overnight, the sample was removed from the furnace, weighed, and acid-cleaned. The solid alloy charge was then sectioned into samples for carbon analysis by using a diamond saw. Between three and five of these sectioned samples were acid-cleaned and analyzed for carbon content.

The relative importance of coating reaction [Reaction (2)] and inleakage [Reactions (6) and (7)] during foundry operations was investigated by using modifications of the procedure described in the preceding paragraph. Yttria, coated-yttria, and coated-graphite crucibles were used to determine carbon contributions from the binder and from coating-graphite reactions. After uranium samples were loaded into the furnace and evacuated, the temperature profile shown in Fig. 1 was used to simulate foundry heating cycles of the liquid metal. Air was also substituted for CO during an inleakage experiment to evaluate foundry vacuum conditions.

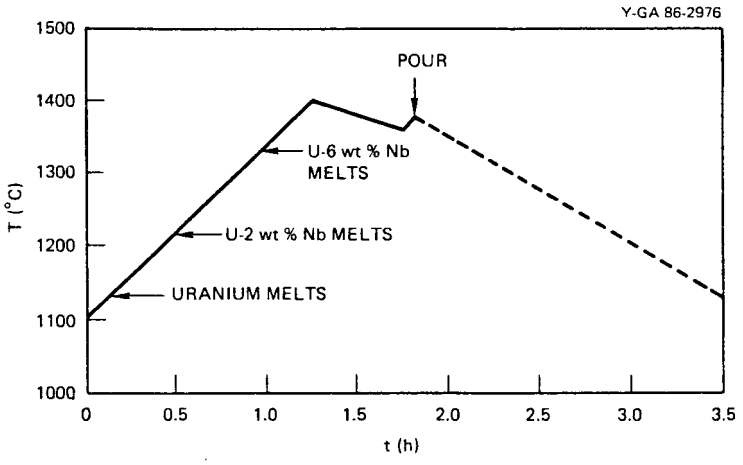

Fig. 1. Temperature-time profile used to simulate foundry furnacing. The arrow at 1.8 h indicates when the melt would be poured in the foundry. In these simulations, heat is reduced at this time and the profile shown by the dashed line is thus produced. Alloy melting points are indicated by arrows.

RESULTS

CARBON MONOXIDE REACTION KINETICS

The experimental results from the parametric study of liquid uranium exposure to CO are summarized in Table 1, which gives for each experiment the exposure time, t (h); the exposure temperature, T (°C); the exposure pressure, [CO] (mtorr); and the specific surface area, S/V (cm^{-1}). The change in carbon content after furnacing, ΔC (ppm), is also listed, along with the standard error in this value. Similar results for the parametric study of the U–6 wt % Nb alloy are summarized in Table 2.

Figures 2 through 5 show the variations in carbon pickup, ΔC, as functions of specific surface area, exposure time, CO pressure, and exposure temperature, with all other variables held constant. In each figure the circles and squares are the respective results for uranium and U–6 wt % Nb alloy reactions with CO at the experimental conditions described in the figure caption. The solid lines in each figure are empirical analyses of the form

$$\Delta C = a[CO]^b t^c (S/V)^d \exp[e/(T + 273.15)] \quad . \qquad (8)$$

where parameters a, b, c, d, and e were determined by pairwise regression analysis of Eq. (6) with the appropriate dependent and independent variables.[4]

Table 1. Summary of liquid uranium[a] exposures to carbon monoxide

Run	t (h)	T (°C)	[CO] (mtorr)	S/V (cm^{-1})	ΔC (ppm)
U18	0.50	1410	0.0	2.92	11 ± 2
U19	0.50	1410	5.0	2.89	193 ± 3
U20	0.50	1410	2.0	2.93	149 ± 2
U21	0.50	1410	1.0	3.18	93 ± 3
U22	1.00	1410	20.0	3.13	202 ± 9
U25	1.00	1410	2.0	3.15	120 ± 3
U26	1.50	1410	2.0	3.11	249 ± 3
U27	0.50	1410	2.0	2.78	155 ± 7
U29	0.25	1410	2.0	3.22	99 ± 3
U30	0.10	1410	2.0	2.94	44 ± 2
U31	5.50	1410	2.0	2.76	342 ± 5
U32	0.05	1410	2.0	3.03	44 ± 0
U33	2.50	1410	2.0	2.89	441 ± 6
U34	0.50	1363	5.0	2.90	266 ± 3
U35	0.55	1340	5.0	2.97	250 ± 3
U36	0.50	1276	5.0	3.01	199 ± 2
U37	0.50	1200	5.0	2.86	73 ± 3
U38	0.50	1223	5.0	3.16	116 ± 2
U39	0.50	1290	5.0	2.98	202 ± 4
U40	0.50	1380	5.0	2.73	401 ± 4
U41	0.50	1410	2.0	2.14	217 ± 3
U42	0.50	1410	2.0	1.27	98 ± 2
U43	0.50	1410	2.0	5.53	210 ± 3
U44	0.50	1410	2.0	1.32	82 ± 2
U45	3.00	1410	2.0	2.82	330 ± 4
U47	0.50	1411	2.0	1.32	82 ± 2
U48	0.50	1409	2.0	1.62	93 ± 3

[a]Initial uranium carbon concentration of $[C]_0$ = 76 ± 2 ppm.

Table 2. Summary of liquid uranium–6 wt % niobium alloy[a] exposures to carbon monoxide

Run	t (h)	T (°C)	[CO] (mtorr)	S/V (cm^{-1})	ΔC (ppm)
U58	0.50	1410	5.0	3.95	55
U62	0.50	1450	0.0	2.64	3
U64	0.50	1450	1.0	2.62	35
U65	0.50	1450	2.0	2.60	81
U66	0.50	1450	5.0	2.76	96
U67	0.50	1450	10.0	2.60	123
U68	0.50	1451	20.0	2.61	59
U69	0.52	1449	50.0	2.54	35
U70	1.00	1450	5.0	2.70	40
U71	2.00	1450	5.0	2.61	81
U72	0.25	1451	5.0	2.84	78
U73	0.10	1450	5.0	2.59	43
U74	1.65	1449	5.0	2.64	104
U75	0.50	1472	5.0	2.65	74
U76	0.50	1407	5.0	2.69	48
U78	0.50	1492	5.0	2.59	70
U79	0.50	1382	5.0	2.70	62

[a]Initial alloy carbon concentration of $[C]_0$ = 98 ppm.

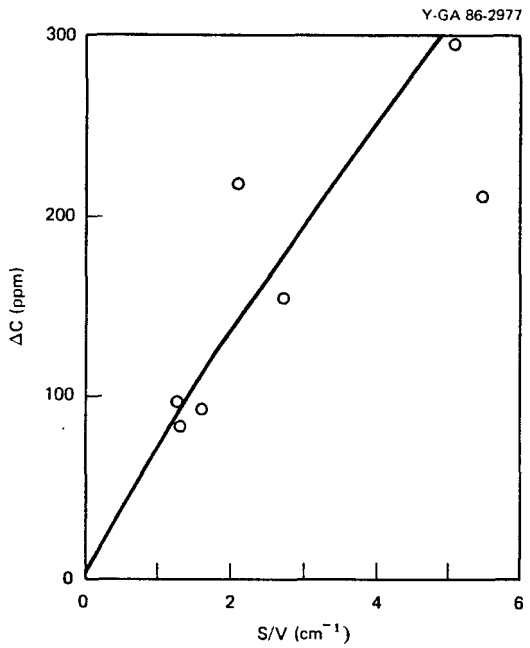

Fig. 2. Uranium carbon pickup, ΔC, as a function of the specific surface area (S/V), at the liquid-vacuum interface. The circles are experimental results obtained from 30-min exposures to 2 mtorr CO at 1410°C. The solid line is a regression analysis of Eq. (8) to the experimental results.

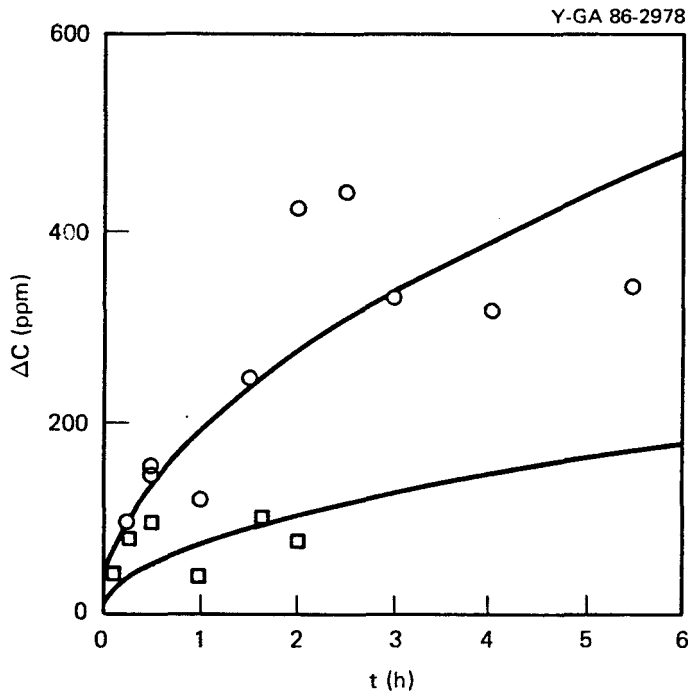

Fig. 3. Carbon pickup, ΔC, as a function of exposure time, t, for uranium and U-6 wt % Nb alloy. The circles are experimental results obtained from uranium exposures to 2.0 mtorr CO at 1410°C. The squares are U-6 wt % Nb alloy exposures to 5.0 mtorr CO at 1450°C. In each case, the specific surface area is ~3 cm^{-1}. The solid line is regression analysis of Eq. (8) to the appropriate experimental results.

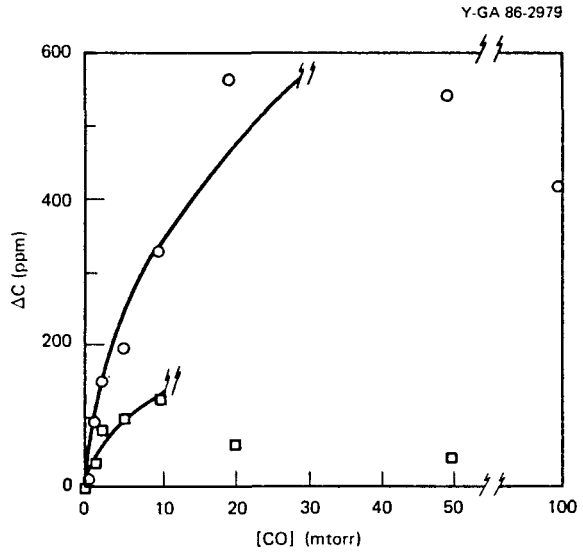

Fig. 4. Carbon pickup, ΔC, as a function of CO pressure, [CO], for uranium and U-6 wt % Nb alloy. The circles are uranium exposures for 30 min at 1410°C. The squares are U-6 wt % Nb alloy exposures for 30 min at 1450°C. The solid line is regression analyses of Eq. (8) to experimental results where [CO] <30 mtorr.

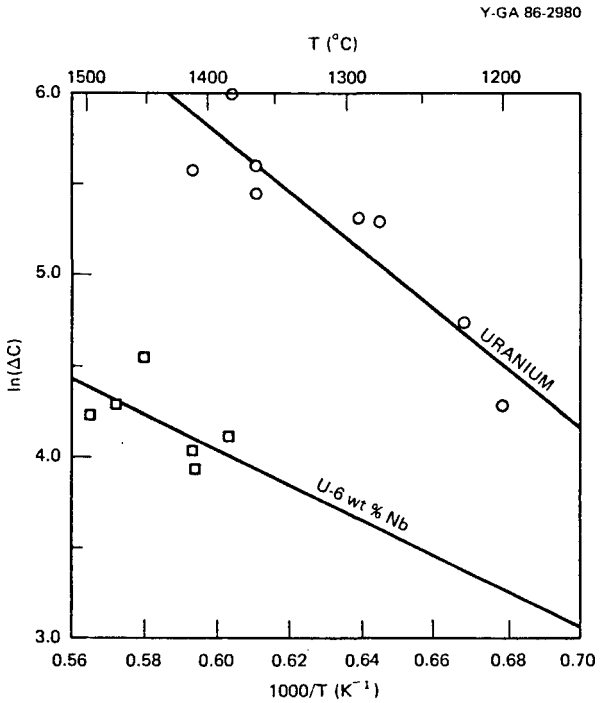

Fig. 5. Arrhenius display of carbon pickup, ΔC, with exposure temperature, T. The circles are experimental results obtained from 30-min uranium exposures to 5.0 mtorr CO. The squares are 30-min exposures of U-6 wt % Nb alloy to 5 mtorr CO. Specific surface area is ~3 cm^{-1}. The solid line is regression analysis of Eq. (8) to the appropriate experimental results.

Regression analysis of carbon pickup with specific surface area, S/V, shown in Fig. 2, yielded d = 0.88 ± 0.14. The large uncertainty in the parameter d is due to the difficulty in accurately measuring the surface area of the gas-liquid interface after the molten sample had cooled. Since the result was within experimental error of the theoretical value (d = 1.00), the carbon pickup was assumed to be proportional to the specific surface area in all subsequent analyses of uranium and U-Nb alloys.

Simultaneous regression analyses of carbon increase with pressure, time, and temperature using the data in Tables 1 and 2, and Eq. (8) yielded the following empirical expressions for uranium and U–6 wt % Nb alloy, respectively:

$$\Delta C = 1.094 \times 10^4 \, [CO]^{0.52} \, t^{0.51} \exp[-9077/(T + 273)] \, (S/V)^1 \, , \quad (9)$$

and

$$\Delta C = 8.78 \times 10^4 \, [CO]^{0.42} \, t^{0.15} \exp[-14949/(T + 273)] \, (S/V)^1 \, , \quad (10)$$

with coefficients of determination $r^2 = 0.78$ and $r^2 = 0.88$, respectively.

Table 3 shows the variation in CO reaction rate for uranium alloys of different niobium compositions. As the niobium concentration in column 1 increases, CO exposures at constant time, temperature, and pressure (columns 2 through 4) produce decreasing carbon contamination, as shown by the normalized carbon pickup [ΔC ÷ (S/V)] in the last column. This reduction is shown graphically in Fig. 6, where the normalized carbon pickup is displayed as a function of niobium concentration. The circles are the results from Table 3, and the solid line is an empirical representation of the experimental results described by

$$[\Delta C \div (S/V)] = 76.8 \exp(-\, 0.28 \times [Nb]) \, , \quad (11)$$

determined by regression analysis ($r^2 = 0.96$).

Table 3. Reactivity of various uranium niobium alloys[a] with carbon monoxide

[Nb] (wt %)	t (h)	T (°C)	[CO] (mtorr)	ΔC ÷ (S/V) (ppm cm)
0.0	0.5	1410	5.0	67 ± 1
1.5	0.5	1410	5.0	61 ± 20
6.0	0.5	1410	5.0	14 ± 2

[a]Initial alloy carbon concentration of $[C]_o$ = 81 ± 2 ppm.

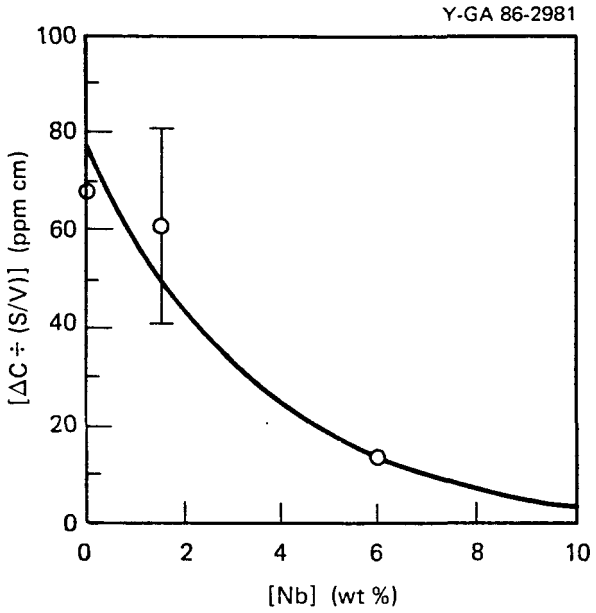

Fig. 6. Normalized carbon pickup, [ΔC ÷ (S/V)] as a function of niobium concentration in uranium. The circles are the experimental results displayed in Table 3; the solid line is a regression analysis described by Eq. (11).

FOUNDRY FURNACING SIMULATIONS

Experimental simulations of foundry heating cycles are summarized in Table 4. The crucible materials; coating materials; total pressure during the run, P (mtorr); and the carbon concentration increase, ΔC (ppm), are given for four experiments. The average specific surface areas (S/V) were 4.39 and 4.86 cm^{-1} for the uranium-vacuum and uranium-crucible interfaces, respectively. A comparison of experiments U51 and U52 indicates that binder decomposition from the yttria paint increased the carbon contamination in uranium by 6 ppm. The yttria-graphite reaction produced an additional 51 ppm carbon concentration increase (U53). Air inleakage of 5 mtorr in experiment U55 increased the carbon concentration by 104 ppm.

Table 4. Carbon contamination in uranium[a] during foundry furnacing simulations

Run	Crucible	Coating	P (mtorr)	ΔC (ppm)
U51	Yttria	None	0.005	68
U52	Yttria	Yttria	0.012	74
U53	Graphite	Yttria	0.016	125
U55	Graphite	Yttria	5.000	229

[a]Initial carbon concentration of $[C]_0$ = 76 ± 2 ppm.

DISCUSSION

KINETIC MECHANISM

The results in Table 1 indicate that the reaction of uranium with CO is significant. As discussed in the preceding section, the variations in ΔC with specific surface area are consistent with experimental uncertainties and theoretical estimates. The time and pressure dependence of carbon increase suggest that CO diffusion across the liquid-vacuum interface may control the reaction rate. A diffusion-controlled mechanism would predict $t^{0.5}$ and $[CO]^{0.5}$ kinetic dependencies. This mechanism is also consistent with the observations (1) that an oxide film forms on the interface after CO exposure (which could retard subsequent CO reaction) and (2) that uranium carbide layers are formed after CO exposures at high pressures and long times. The data are not sufficient, however, to exclude other potential mechanisms. For example, a CO reaction that is limited by oxygen or carbon solubility might also explain the saturation observed at long times and high pressures (observed in Figs. 3 and 4).

The temperature dependence shown by the solid line in Fig. 5 indicates a reaction activation energy E_a= 32 kcal/mol. However, the experimental results indicate some curvature with temperature as compared with predicted Arrhenius behavior. This result may be due to experimental uncertainties or the interaction of different reaction mechanisms over the temperature range.

The results in Tables 2 and 3 show that the CO reaction with the U–6 wt % Nb alloy is approximately three to five times as slow as the reaction with uranium, depending on the exposure conditions, and that the reaction rate decreases with increasing niobium concentration. Within experimental error, the U–Nb alloy reaction also has kinetic dependence consistent with the observation that CO diffusion at the vacuum-liquid interface is the rate-controlling mechanism. The reduction in CO reaction rate with increasing niobium concentration suggests that CO reacts preferentially with uranium [Reaction (4)], even though the niobium carbides (Nb_2C and NbC) are thermodynamically more stable and are the final carbon products in U-Nb alloys.

PROCESS IMPLICATIONS

Uranium-niobium alloy electrodes (3036 castings) are prepared from feed containing 65 to 75 wt % uranium and 25 to 35 wt % U–6 wt % Nb alloy. Since the CO reaction with uranium is three to five times as fast as the CO reaction with the U–6 wt % Nb alloy, ~85 to 95% of the carbon contamination produced from CO reaction is the result of reaction with the pure uranium (derby) charge. Although the uranium feed contains less carbon than the recycled U–6 wt % Nb alloy, the uranium is more reactive with CO during induction furnacing.

The importance of the CO reaction relative to coating-graphite and binder decomposition reactions is illustrated in Table 2. These results must be scaled by the specific surface areas of the uranium-vacuum and

uranium-crucible interfaces of the foundry crucible. For a typical induction furnace casting containing 830 kg of U–2 wt % Nb alloy melted in a 76-cm-ID and 61-cm-tall graphite crucible, the specific surface areas of the vacuum-liquid interface and crucible-liquid interface are 0.128 and 0.149 cm^{-1}, respectively. Since the coating binder decomposition and coating-graphite reaction contributions should scale with the crucible-liquid interface area, the results in Table 2 indicate that binder decomposition should increase casting carbon concentrations by 0.2 ppm.

Similar analysis indicates that the coating-graphite reaction should increase foundry casting carbon levels by 1.5 ppm. This estimate is in remarkably good agreement with Holcombe's TGA estimates that predict carbon contamination of 2.4 ppm if all CO generated by Reaction (2) reacts with the uranium.[2,5] Comparison of these two results suggests that ~63% of the CO generated at the coating-uranium interface reacts with the melt. The remainder of the CO generated at this interface either diffuses (with no reaction) through the uranium or diffuses out through the graphite crucible.

The results in Table 4 also indicate that the CO-U reaction should increase uranium melt carbon content by 3.0 ppm at a furnace pressure of 5 mtorr. Because foundry furnaces operate at a nominal pressure of 170 ± 65 mtorr, the CO reaction should be even more important to foundry carbon contamination. Equation (7) predicts that the CO-U reaction will increase with $[CO]^{0.52}$. Therefore, if [CO] in the foundry furnaces is assumed to be proportional to the total pressure, the result in Table 2 predicts that the CO-U reaction will increase uranium carbon contamination by 19 ppm. Since uranium comprises ~70% of the 3036 charge, a carbon pickup of 13 ppm is expected from the CO-U reaction. Another 2 or 3 ppm carbon pickup is expected from the CO reaction with U–6 wt % Nb alloy. Thus, the total casting carbon pickup from the CO reaction is 16 ppm. Comparison of the various carbon contamination mechanisms at nominal foundry conditions indicates that the CO-U reaction is 10 times as important as the coating-graphite reaction and 75 times as important as binder decomposition.

Carbon contamination during foundry operation can be used together with Eq. (9) to provide an estimate of CO pressure in the furnace. Assuming that no CO-U reaction occurs below 1100°C and that the CO pressure remains constant during furnacing, Eq. (9) can be numerically integrated to give

$$\Delta C = 2483\ (S/V)\ [CO]^{0.52}\ , \tag{12}$$

for the temperature profile shown in Fig. 1. For a typical induction furnacing, $S/V = 0.128\ cm^{-1}$ and Eq. (12) becomes

$$\Delta C = 318\ [CO]^{0.52}\ . \tag{13}$$

Equation (13) can be used to estimate CO pressures for various levels of carbon contamination in the foundry furnace. For ΔC = 16 ppm, Eq. (13) predicts that [CO] = 0.003 mtorr. Thus, carbon contamination in the vacuum induction furnace should be very sensitive to low CO partial pressures.

This result, together with the facts that large quantities of other gases are present and that [CO] is not monitored in foundry operation, makes direct observation of the CO reactions difficult. Since typical foundry melting operations add approximately 35 ppm carbon into the 3036 castings, the CO reactions may be responsible for almost half the carbon addition. However, CO comprises less than 0.01% of the total gas present in the furnace, the remainder being nitrogen, oxygen, and hydrogen from air inleakage and gas reactions in the furnace. These gases not only make detection of CO difficult but they may also complicate the CO-U alloy reaction by partially passivating the uranium surface. (Nitrogen passivation of liquid uranium alloys is currently being investigated.

Although direct evidence of the CO-U reaction is difficult to observe in typical foundry operations, foundry runs in which vacuum inleakage occurs demonstrate the importance of the CO-U reaction. For example, in the production of a 3036 casting for which the total furnace pressure approached 2800 mtorr, the carbon content of the casting increased by 102 ppm rather than the usual 34 ppm. Assuming that the CO partial pressure was proportional to total pressure, P, and that carbon contamination from the CO reaction increases with the power of 0.52 of [CO], carbon contamination from the CO-U reaction during this foundry operation is empirically described by

$$\Delta C = 1.13\ [P]^{0.52}\ . \qquad (14)$$

If Eq. (14) is used to estimate the CO contribution at typical foundry furnace pressures (170 mtorr), a prediction of 16 ppm carbon contamination produced by CO is obtained. Equation (14), though derived by analysis of a high-pressure foundry run, is in remarkably good agreement with the CO contribution predicted from the laboratory results in Table 2 and Eq. (12).

The preceding analyses indicate that the reaction of CO at the liquid-vacuum interface is a major source of carbon contamination during foundry induction furnacing, probably responsible for almost half the carbon contamination produced in routine casting operations. Both laboratory and actual production data are in remarkably good agreement in estimating the importance of this reaction. Therefore, attempts to reduce carbon contamination during foundry operations must include this reaction. Potential methods of controlling this reaction could address each of the independent variables in Eq. (9): CO pressure, exposure time, exposure temperature, and liquid-vacuum interface area. Of these four variables, specific surface area of the liquid-vacuum interface and CO pressure during furnacing appear to be most easily changed in foundry operation. The liquid-vacuum interface could be reduced by changing the crucible dimensions or by melting more alloy during foundry runs ("double" casting). Similarly, CO pressure could be reduced by improving furnace vacuum.

CONCLUSIONS

A parametric study of the CO reaction with liquid uranium and liquid U-Nb alloys as functions of niobium concentration, CO pressure, furnacing time, furnace temperature, and specific liquid-vacuum interface area indicates that this reaction is a major source of carbon contamination in foundry operations. Both laboratory and production data indicate that this reaction is responsible for approximately half the carbon contamination introduced in the production of 3036 castings. Reaction kinetics are consistent with CO diffusion through an oxide film at the liquid-vacuum interface as the rate-determining step. Comparison of the various carbon contamination mechanisms at typical foundry conditions indicated that the CO-U reaction is 10 times as important as the coating-graphite reaction and 75 times as important as contributions from binder decomposition. Reduction of carbon contamination in this operation will require reductions in casting temperature, alloy surface area, or furnace pressure.

ACKNOWLEDGMENTS

The authors thank L. R. Chapman, R. T. Palmer, and P. A. McSorley for the analysis of foundry operation and for many helpful discussions and J. E. "Tommy" Thompson, Jr., for making the foundry facilities available for observation and analysis.

REFERENCES

1. W. D. Wilkinson, *Uranium Metallurgy*, vols. 1 and 2, Interscience, New York, 1962.

2. J. B. Condon and C. E. Holcombe, Jr., *Crucible Materials to Contain Molten Uranium,* Y-2082; Union Carbide Corp. Nuclear Div., Oak Ridge Y-12 Plant, September 1977.

3. R. H. Reiner and C. E. Holcombe, Jr., *Carbon Monoxiode Interaction with Liquid Uranium*, Y/DU-485, Martin Marietta Energy Systems, Inc., Oak Ridge Y-12 Plant, April 1986.

4. Brice Carnahan and H. A. Luther, *Applied Numerical Methods*, John Wiley and Sons, New York, 1962, p. 572.

5. J. B. Condon and C. E. Holcombe, Jr., "Kinetics of the Yttria-Carbon Reaction," *High Temperature Science* **18**, 79–95 (1984).

DISTRIBUTION

Department of Energy - Oak Ridge

Poteat, R. M.
Spence, R. J.

Lawrence Livermore National Laboratory

Clough, R. E./Galles, H. L.
Miller, G. H.
Ragaini, R. C.
Robbins, J. L.
Sanford, C. B.
Shuler, W. B./Wraith, C. L.
Technical Information Division
Werne, R. W./Grissom, M. L.

Los Alamos National Laboratory

Hoyt, H. C.

Oak Ridge Y-12 Plant

Beck, D. E.
Burditt, R. B.
Chapman, L. R.
Clift, J. H.
Dodson, W. H.
Googin, J. M.
Holcombe, C. E., Jr.
Keith, A.
Keyser, R. M.
Kite, H. T.
Koger, J. W.
Lomax, B. A.
Long, C. J.
McElroy, B. D.
Mills, J. M., Jr.
Montgomery, C. D.
Northcutt, W. G., Jr.
Palmer, R. T.
Reiner, R. H. (20)
Schede, R. W.
Smyrl, S. L.

Thompson, J. E., Jr.
Walton, Y. W.
Y-12 Central Files (master copy)
Y-12 Central Files (route copy)
Y-12 Central Files (Y-12 RC)
Y-12 Central Files (5)

Paducah Gaseous Diffusion Plant

Walter, C. W.

Sandia National Laboratories - Livermore

Olson, D. M.

In addition, this report is distributed in accordance with Categories UC-4, **Chemistry,** and UC-25, **Materials,** as given in the *Standard Distribution for Unclassified Scientific and Technical Reports*, DOE/TIC-4500.